

Direct observation of two-step polarization reversal by an opposite field in a substrate-free piezoelectric thin sheet

Chun-Yi Hsieh,¹ Yang-Fang Chen,¹ Wan Y. Shih,² Qing Zhu,³ and Wei-Heng Shih^{3,a)}

¹Department of Physics, National Taiwan University, Taipei 106, Taiwan

²School of Biomedical Engineering, Science, and Health Systems, Drexel University, Philadelphia, Pennsylvania 19104, USA

³Department of Materials Science and Engineering, Drexel University, Philadelphia, Pennsylvania 19104, USA

(Received 30 November 2008; accepted 24 February 2009; published online 31 March 2009)

The domain switching behavior of a substrate-free lead magnesium niobate-lead titanate thin sheet by an opposite electric field (E) was examined by piezoresponse force microscopy. It is shown that the polarization reversal process involved two steps. First, the polarization switched from the initial normal direction to an in-plane direction at $-E < 5$ kV/cm. Second, at $-E > 5$ kV/cm, the polarization was further switched from the in-plane direction to the opposite field direction. The preference of the in-plane polarization at -5 kV/cm was attributed to the thin-sheet geometry, which also manifested itself as a maximum in dielectric constant at the same field. © 2009 American Institute of Physics. [DOI: 10.1063/1.3107264]

A major recent development in perovskite piezoelectric oxides was the orientation-enhanced piezoelectric response in specially cut lead magnesium niobate-lead titanate (PMN-PT) and lead zinc niobate-lead titanate (PZN-PT) single crystals.^{1,2} With a rhombohedral composition near a morphotropic phase boundary, (001) PMN-PT single crystals can exhibit a d_{33} coefficient more than three times higher than that of the bulk. More recently, an analogous giant piezoelectric enhancement was also observed in 8 and 22 μm thick polycrystalline $[\text{Pb}(\text{Mg}_{1/3}\text{Nb}_{2/3})\text{O}_3]_{0.63}[\text{PbTiO}_3]_{0.37}$ (PMN-37PT) thin sheets processed and sintered without a substrate (substrate-free thereafter).^{3,4} *In situ* x-ray diffraction indicated that these substrate-free PMN-37PT thin sheets retained a large fraction of a -domains with an in-plane polarization direction even after poling. The observed preference of a -domains in the PMN-37PT thin sheets was attributed to the depolarization effect of the thin-sheet geometry. This behavior is markedly different from the predominance of c -domains with a normal polarization observed in ferroelectric thin film capacitors such as $\text{Pb}(\text{Zr}_{0.2}\text{Ti}_{0.8})\text{O}_3$ grown on a substrate⁵⁻⁸ where a -domains mainly existed in twin boundaries.^{6,9} In an electric field opposite to the poling direction, these ferroelectric $\text{Pb}(\text{Zr}_{0.2}\text{Ti}_{0.8})\text{O}_3$ films underwent straight 180° polarization reversal. Several piezoresponse force microscopy (PFM) studies have been devoted to examining the kinetics of this polarization reversal process in an opposite field⁵⁻⁸ and were extended to ferroics such as BiFeO_3 .^{10,11} Since the PMN-37PT thin sheets do not have the clamping effect of a substrate, it is likely that the polarization reversal process of these substrate-free PMN-37PT thin sheets would be quite different from that of films grown on a substrate that exhibit predominantly c -domains.

The purpose of this study is to examine the polarization switching behavior of polycrystalline PMN-37PT thin sheets at a single grain level in an opposite electric field by measuring the vertical piezoelectric response (VPFM) as well as the lateral piezoelectric response (LPFM) simultaneously us-

ing the PFM technique. The PMN-37PT sheet was 8 μm thick made first by dispersing crystalline lead magnesium niobate $\text{Pb}(\text{Mg}_{1/3}\text{Nb}_{2/3})\text{O}_3$ (PMN) powders made from a colloidal coating approach^{12,13} in a lead titanate precursor solution containing lead acetate and titanium isopropoxide in ethylene glycol to yield a PMN-37PT precursor powder with a nominal 10% lead excess. After drying at 300 $^\circ\text{C}$, the PMN-37PT precursor powders were mixed with a proprietary dispersing resin and ball milled in an alcohol/ketone mixture for 24 h followed by the addition of the remaining portion of the resin along with a phthalate-based plasticizer and ball milling for an additional 24 h. The slurry was then deaired, and cast into the desired thickness and sintered in a doubly covered Al_2O_3 crucible at 1000 $^\circ\text{C}$ for 2 h.¹⁴

PFM measurements were carried out using a modified scanning probe microscope (Stand Alone SMENA apparatus, NT-MDT) equipped with a platinum-iridium coated silicon tip (electrostatic force microscopy-PtIr5 coating, Nanoworld). A function generator (DS345, Stanford Research System) provides an alternating current (ac) voltage of 1 V operated at 15 kHz between the tip and the bottom electrode on the back side of the PMN-37PT sheet for PFM measurements and an additional direct current (dc) bias voltage to generate a dc bias electric field in the sample. Both the VPFM, which was proportional to the vertical component of the polarization and the LPFM, which was proportional to the lateral component of the polarization as schematically shown in Fig. 1(a), were recorded using a lock-in amplifier (SR830, Stanford Research System).⁴ Note that the LPFM only measures the polarization along one lateral direction [y -direction in Fig. 1(a)] and misses the polarization that points in the x -direction. To examine the domain switching behavior in an opposite electric field, the sample was first scanned with a 12.5 kV/cm dc bias field. Subsequently, the VPFM and LPFM were scanned with an opposite bias field of -1.25 , -2.5 , -5 , -7.5 , -10 to -12.5 kV/cm.

Figure 1(b) shows the topographic image of a $5 \times 5 \mu\text{m}^2$ area of an 8 μm thick PMN-37PT thin sheet. The grain marked by the dash square was studied by PFM. Figure

^{a)}Electronic mail: shihwh@drexel.edu.

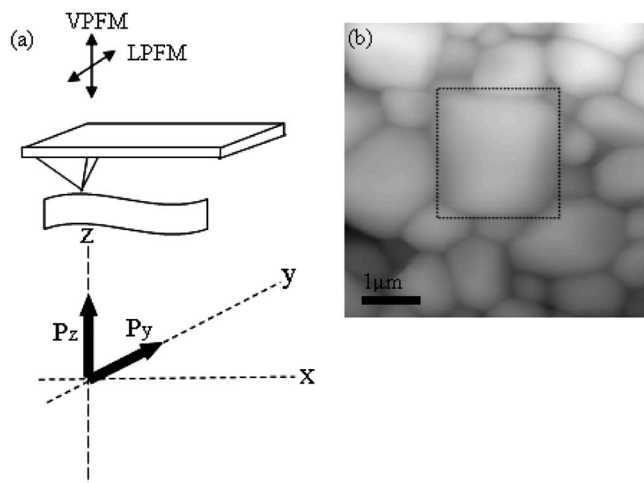


FIG. 1. (a) A schematic of the PFM and (b) an atomic force microscopy image of the 8 μm PMN-37PT thin sheet. The dash square in Fig. 1(b) shows the region where the detailed PFM measurements were carried out. The VPFM correlates with the vertical component of the polarization while the LPFM with the lateral component of the polarization along the width direction of the PFM probe.

2 shows the VPFM and LPFM images of the dash square in Fig. 1(b) at various electric fields. From Figs. 2(a) and 2(e), at $E=12.5$ kV/cm, the VPFM image was bright and the LPFM image was dark indicating the polarization was mostly aligned with dc bias field. As the bias electric field was reduced to zero, the VPFM was reduced and the LPFM increased producing domain patterns of alternating bright and dark stripes in both the VPFM [Fig. 2(b)] and LPFM [Fig. 2(f)] images. Figures 2(c) and 2(g) show the VPFM image and the LPFM image obtained at an opposite field of

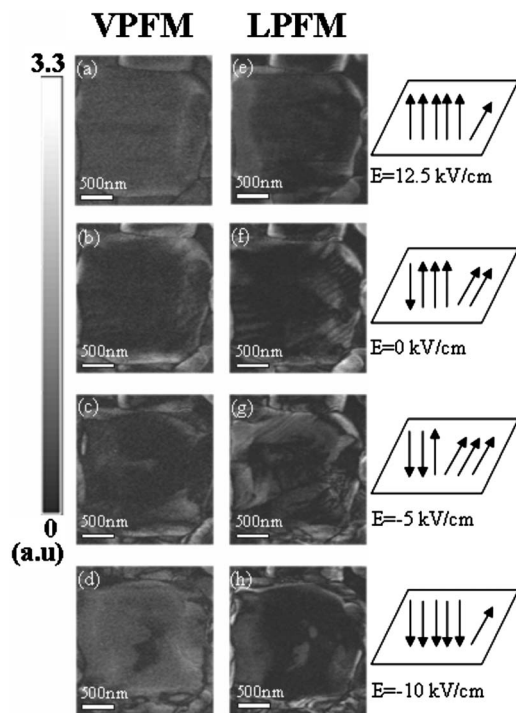


FIG. 2. VPFM images of the inset of Fig. 1(b) at (a) 12.5 kV/cm, (b) 0 kV/cm, (c) -5 kV/cm, and (d) -10 kV/cm and the LPFM of the same region at (e) 12.5, (f) 0, (g) -5 , and (h) -10 kV/cm. The vertical scale bar indicates the magnitude scale. The right-hand column shows the schematics of the domain switching sequence as an opposite field is applied to the PMN-PT sheet.

$E=-5$ kV/cm. As can be seen, the LPFM became brighter than at zero field [Fig. 2(g)] and the VPFM became darker than at zero field [Fig. 2(c)] indicating switching of the polarization direction from the normal to an in-plane direction. When the bias electric field further changed from -5 to -10 kV/cm, the VPFM became brighter [Fig. 2(d)] and the LPFM darker [Fig. 2(h)] indicating the polarization switched from an in-plane to a normal direction. The results shown in Figs. 2(a)–2(h) indicate that the polarization reversal of a PMN-37PT thin sheet in an opposite electric field involved two steps. The polarization first switched from a normal to an in-plane direction at fields around -5 kV/cm as evidenced by the decrease in VPFM and increase in LPFM. The second step involved switching the polarization from an in-plane direction to a normal direction in the negative field direction. To illustrate the steps, the sequence of the polarization switching is shown in schematics in the right column of Fig. 2. The detailed mechanism of the two-step domain switching process is beyond the scope of the present paper and can only be speculated here. In typical situation where a substrate is present, 180° domain switching would be preferred because the substrate prohibits any switching that involves lateral strain. However, in the present substrate-free film geometry the lateral strain in the planar direction is allowed. Furthermore, the preference of the in-plane polarization may provide a local minimum in free energy in polarization causing the 90° domain switching from the normal polarization to the in-plane polarization at low opposite electric fields. At a higher opposite electric field, a second 90° domain switching causes the in-plane polarization to switch to the opposite normal polarization. More studies are needed to clarify this mechanism.

Since both the VPFM and the LPFM were not uniform in space, we plot the VPFM and LPFM distributions at various bias electric fields in Figs. 3(a) and 3(b), respectively. The peak magnitude of the VPFM first decreased from around 0.6 at $E=12.5$ kV/cm to about 0.3 at $E=0$ and -5 kV/cm. After that it reversed the trend and increased to about 0.7 at $E=-10$ kV/cm. In Fig. 3(b), the LPFM first broadened its distribution to higher LPFM values at $E=-5$ kV/cm due to the emergence of more a -domains at this field and the distribution narrowed to a lower LPFM range at $E=-10$ kV/cm as in-plane polarization switched to the normal direction. Using these distributions in Figs. 3(a) and 3(b), we obtained the average VPFM and LPFM over the scanned area at each electric field shown in Fig. 4(a). The average VPFM exhibited a minimum at around $E=-5$ kV/cm and the average LPFM exhibited a maximum at around -5 kV/cm. The behavior in Fig. 4(a) supports that in-plane polarization was preferred in these PMN-37PT thin sheets even in an opposite electric field. Only with a large enough opposite field one could switch the polarization direction to align with the opposite electric field. We also monitored the phase of VPFM and LPFM at a few locations. It was observed that at $E\sim-5$ kV/cm where the amplitude of VPFM exhibited a minimum the phase of VPFM underwent a rapid change from -88° at $E=0$ kV/cm to 21° at -5 kV/cm, to 63° at $E=-6$ kV/cm. On the other hand, the phase of LPFM remained more or less the same as the field was changed from positive to negative.

The domain switching behavior as shown in Figs. 2(a)–2(h) and Figs. 3(a) and 3(b) at the single grain level can manifest itself in macroscopic measurements such as width-

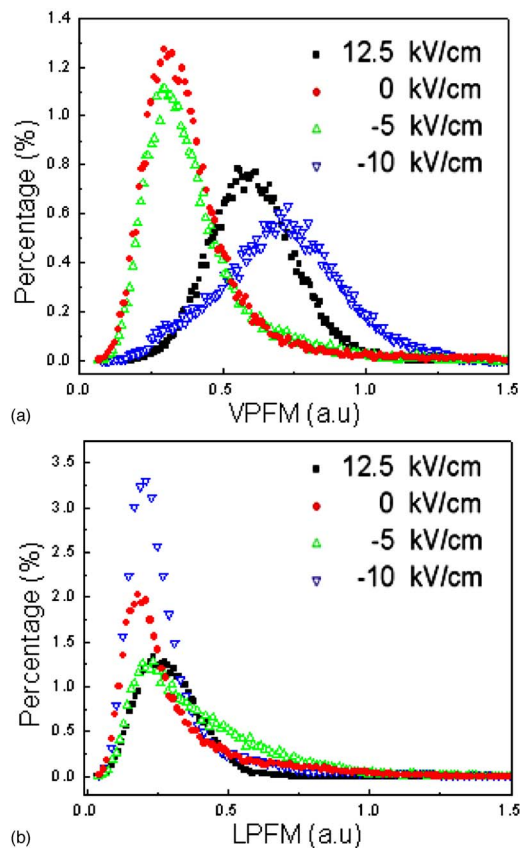


FIG. 3. (Color online) Distribution of (a) VPFM and (b) LPFM at different applied fields.

mode resonance frequencies¹⁵ and dielectric constant of the PMN-37PT sheet. As an example, Fig. 4(b) shows the relative change in the dielectric constant of a poled PMN-37PT sheet versus the bias electric field. The sample shown in Fig. 4(b) was poled at 15 kV/cm at 80 °C on a hot plate for 30 min and aged for 1 day before the measurement. As can be seen, the relative dielectric constant exhibited a maximum at -5 kV/cm. The maximum in the dielectric constant shown in Fig. 4(b) was consistent with the maximum average LPFM at this field. It is known that *a*-domains of PMN-PT exhibited a higher dielectric constant than the *c*-domains.¹⁶ Consequently, the maximum average LPFM at -5 kV/cm, indicating the largest population of *a*-domains, results in a maximum in dielectric constant.

In summary, we have examined the domain switching behavior of an 8 μm thick PMN-37PT thin sheet produced without a substrate in an opposite electric field. Unlike ferroelectric films deposited on a substrate with predominant *c*-domains that exhibit straight 180° polarization reversal in an opposite field, the PMN-37PT thin sheet exhibited a two-step polarization reversal in an opposite field. First, the polarization switched from the normal to an in-plane direction at $-E < 5$ kV/cm. At $-E > 5$ kV/cm, the in-plane polarization switched to the normal direction aligning with the opposite field to complete the polarization reversal. The preference of the *a*-domains in the -5 kV/cm $< E < 0$ was attributed to the depolarization effect of the thin-sheet geometry and manifested itself in the maximum relative dielectric constant change measured at $E = -5$ kV/cm.

This work is supported by Grant No. NSC94-2112-M-002-006 from the National Science Council of Republic of

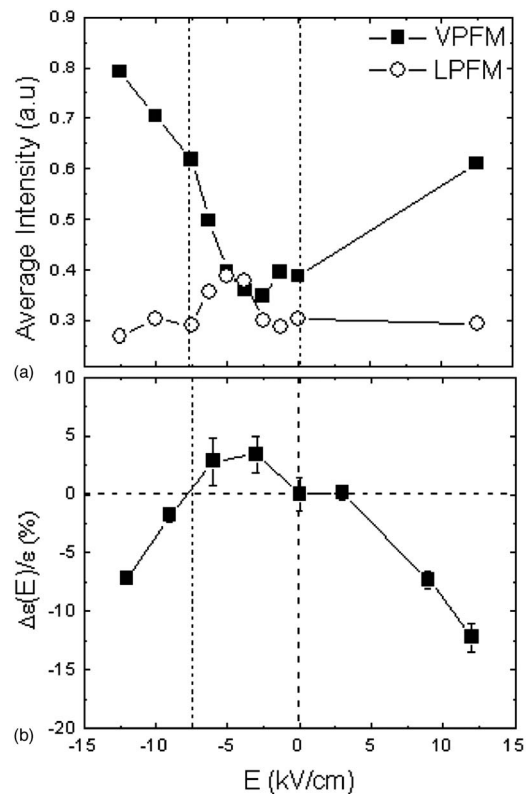


FIG. 4. (a) The average VPFM and LPFM vs applied field, (b) relative dielectric constant change of the PMN-37PT thin sheet vs electric field. Note the correlation between the peak in LPFM and the peak in relative dielectric constant change at -5 kV/cm.

China and in part by the National Institute of Biomedical Imaging and Bioengineering (NIBIB), National Institute of Health (NIH) through Grant No. RO1EB00720-02, and Nanotechnology Institute of Southeastern Pennsylvania. We also thank Mr. Wei-Hung Liu and Dr. Wei-Sheng Su for their help in the PFM study.

¹Data of commercially available products, APC International, Ltd.

²S.-E. Park and T. R. Shrout, *J. Appl. Phys.* **82**, 1804 (1997).

³W. Y. Shih, H. Luo, C. Martorano, H. Li, and W.-H. Shih, *Appl. Phys. Lett.* **89**, 242913 (2006).

⁴W.-S. Su, Y.-F. Chen, W. Y. Shih, H. Luo, and W.-H. Shih, *Appl. Phys. Lett.* **91**, 112903 (2007).

⁵S. Hong, E. L. Colla, E. Kim, D. V. Taylor, A. K. Tagantsev, P. Murali, K. No, and N. Setter, *J. Appl. Phys.* **86**, 607 (1999).

⁶A. Roelofs, N. A. Pertsev, R. Waser, F. Schlaphof, L. M. Eng, C. Ganpule, V. Nagarajan, and R. Ramesh, *Appl. Phys. Lett.* **80**, 1424 (2002).

⁷S. M. Yang, J. Y. Jo, D. J. Kim, H. Sung, T. W. Noh, H. N. Lee, J.-G. Yoon, and T. K. Song, *Appl. Phys. Lett.* **92**, 252901 (2008).

⁸A. Gruverman, B. J. Rodriguez, C. Dehoff, J. D. Waldrep, A. I. Kingon, R. J. Nemanich, and J. S. Cross, *Appl. Phys. Lett.* **87**, 082902 (2005).

⁹G. Le Rhun, I. Vrejoiu, and M. Alexe, *Appl. Phys. Lett.* **90**, 012908 (2007).

¹⁰P. Maksymovych, S. Jesse, M. Huijben, R. Ramesh, A. Morozovska, S. Choudhury, L.-Q. Chen, A. P. Baddorf, and S. V. Kalinin, *Phys. Rev. Lett.* **102**, 017601 (2009).

¹¹S. V. Kalinin, B. J. Rodriguez, S. Jesse, P. Maksymovych, K. Seal, M. Nikiforov, A. P. Baddorf, A. L. Kholkin, and R. Proksch, *Mater. Today* **11**, 16 (2008).

¹²H. Gu, W. Y. Shih, and W.-H. Shih, *J. Am. Ceram. Soc.* **86**, 217 (2003).

¹³H. Luo, W. Y. Shih, and W.-H. Shih, *Int. J. Appl. Ceram. Technol.* **1**, 146 (2004).

¹⁴H. Luo, Ph. D. thesis, Drexel University (2005).

¹⁵Q. Zhu, W. Y. Shih, and W.-H. Shih, *Appl. Phys. Lett.* **92**, 033503 (2008).

¹⁶F. Xu, S. Trolrier-McKinstry, W. Ren, and B. Xu, Z.-L. Xie and K. J. Hemker, *J. Appl. Phys.* **89**, 1336 (2001), and references therein.